This is a repository copy of *Validation of a novel virtual reality platform for investigating pedestrian-pedestrian interaction in the context of structural vibration serviceability*.

White Rose Research Online URL for this paper:
https://eprints.whiterose.ac.uk/213665/

Version: Published Version

VALIDATION OF A NOVEL VIRTUAL REALITY PLATFORM FOR INVESTIGATING PEDESTRIAN-PEDESTRIAN INTERACTION IN THE CONTEXT OF STRUCTURAL VIBRATION SERVICEABILITY

Artur A. Soczawa-Stronczyk[1], Mateusz Bocian[1,2]

[1] School of Engineering, University of Leicester, UK
e-mail: {aamss1, m.bocian}@leicester.ac.uk

[2] Biomechanics & Immersive Technology Laboratory, University of Leicester, UK

Abstract. Pedestrian-pedestrian interaction (PPI) is one of the fundamental mechanisms purported to influence the amplitudes of structural response under the action of a walking crowd. This is because a pedestrian is likely to alter their gait due to the presence of other pedestrians, which in turns alters the magnitude of structural loading. However, little empirical data are currently available to assess the effect of PPI in the context of vibration serviceability. This is mainly due to logistical challenges in assembling and instrumenting a crowd of walking pedestrians, and the associated cost. To this end, a novel virtual reality platform is developed for experimental investigation of pedestrian-pedestrian interaction. In comparison to real-world crowd testing, the platform enables experimental protocols to be implemented repeatedly in a highly controlled environment while collecting a rich set of data on pedestrian behaviour. The platform incorporates state-of-the-art technology for motion capture, artificial intelligence and three-dimensional computer modelling, and comprises of three core modules: (i) the environment, (ii) the crowd and (iii) the user interface enabling real walking behaviour. To assess the validity of the platform for investigating PPI, tests were conducted to quantify gait synchronisation between a pair of walking pedestrians. The pair of pedestrians consisted of either two real humans or a real human and an avatar generated within a fully immersive VR environment. The test subject was either not explicitly asked to or specifically asked to synchronise their gait while walking side-by-side or front-to-back. It was found that walking with an avatar yields qualitatively the same results as walking with a real person, whether that is with or without the instruction to synchronise gait. However, the results differ quantitatively in terms of the synchronisation strength and the directionality.

1 INTRODUCTION

In recent years, the industry-wide trend of pushing boundaries in terms of sleek and slender design using light materials often leads to reduced mass, stiffness and damping [1] of the newly built structures. As a consequence, several footbridges failed to satisfy the vibration serviceability criteria when occupied by a crowd of people [2–11]. A number of dynamic force models were put forward to account for the adaptation of pedestrian's stepping behaviour due to the presence other walkers [12–15], known as pedestrian-pedestrian interaction (PPI). However, very few studies attempted to uncover the underlying network of complex dynamic interactions present in a crowd of walking pedestrians and quantify the strength of PPI in the context of structural dynamics [16–18]. This is predominantly due to many uncertainties associated with a full-scale crowd testing, but also low repeatability of experimental conditions and a significant logistical challenge of gathering and instrumenting a group of walkers together with the accompanying costs.

To alleviate these issues, a novel experimental platform is proposed to limit the logistical efforts in investigating PPI whilst providing an accurate representation of real-life environment. This is achieved by employing the latest developments in motion capture, three-dimensional modelling and virtual reality (VR) technology, and by using artificial intelligence (AI) - driven virtual pedestrians capable of simulating complex social interactions present in real crowds.

This paper is structured as follows: Section 2 describes the development of the VR experimental platform for PPI investigation, Section 3 details the validation procedure of the platform, followed by the data analysis process, Section 4 presents the validation results together with the discussion, and Section 5 provides the conclusions.

2 DEVELOPMENT OF THE VIRTUAL-REALITY PLATFORM

A construction of biomechanically representative, virtual reality-based experimental platform for investigating PPI consisted of the following stages. Firstly, an optical motion capturing system was employed to record multiple gait cycles of a real person walking with various speeds along a straight line as well as along an arc of circles with various radiuses, with the procedure repeated at multiple walking speeds. Secondly, the recorded motions were used to create an animation controller which would drive the motion of a realistic humanoid character in VR, referred to as an agent. Lastly, a novel AI system was employed to steer the agent in the virtual setting.

2.1 Motion capture

A twenty-five years old male performer (height 182.5 cm, weight: 80 kg) was recruited from the university cohort. He was outfitted with a motion capture equipped with thirty-seven reflective markers placed on body landmarks. The performer was asked to complete four different types of walks at pacing frequencies ranging from 1.3 Hz to 2.0 Hz at 0.1 Hz increments. The walks consisted of walking along a straight line, and around small, medium and large circles with the radiuses of 63.5 cm, 27 cm and 254 cm (25 in, 50 in and 100 in) respectively. A metronome was used to ensure the consistent pacing frequency of the performer throughout the motion recording process.

The gait cycles were recorded using a set of eight OptiTrack Prime 13 cameras, which provided near real-time tracking data at the sampling rate of 120 Hz. The raw tracking data were transferred over to the processing unit over the IEEE 802.3 compliant, gigabit network. The

data were recorded and post-processed using OptiTrack's proprietary software, Motive:Body 2.0.

The initial post-processing consisted of interpolation of missing markers' trajectories due to occlusions and light reflections. Based on the characteristics of the specific marker's trajectory, this was done by employing a first or third-degree polynomial interpolation algorithm. Furthermore, any noise in the raw tracking data was removed by using a fourth-order two-way Butterworth low-pass filter with the cut off frequency at 6 Hz. The primary noise source was markers' vibration, as they were not directly attached to the bones. Also, changes in air temperature and lighting conditions contributed to the decrease in the tracking quality.

The actual processing of the motion capture data was conducted in Autodesk MotionBuilder 2018. During this stage, the original data were down sampled to 30 frames per second. Furthermore, details such as feet's floor contact and fingers positions were adjusted. Finally, from multiple recordings of the same kind, gait cycles were extracted and stitched together to minimise the repeatability of the avatar's motions.

2.2 Avatars creation

Adobe Fuse CC 1.2 was used to create three-dimensional models of humanoid characters employed in VR. The software allowed physical and visual features of virtual avatars to be adjusted, i.e. dimensions of body parts, facial expression and clothing. In order to create the bone structure of the virtual characters, the models were exported to Adobe Mixamo where they were rigged. This created a puppet-like animation mechanism by tying the skeleton to the skin mesh.

Rigged avatars were then exported to Unity 2018.4.0f1 – a game engine used throughout this project. Unity was chosen predominantly due to its C# scripting API and a vast Asset Store collection compared to other game engines.

The next step consisted of retargeting motion-captured gait cycle animations onto the avatars and creating an animation controller. The animation controller employed two-dimensional linear animation blending to create smooth transitions between recorded animations based on two input parameters: (i) selected pacing frequency and (ii) the desired direction of progression.

Footsteps sound effects were added to avatars to provide realistic auditory ques based on the walking surface. The sound effects were programmed to be triggered by every heel strike.

2.3 Steering system

Polarith AI system was implemented to navigate the avatar around the virtual environment by feeding input parameters into the animation controller. It is an artificial-intelligence navigation system which is fully programmable and operates based on a multi-objective optimisation algorithm. The system works in two stages. Firstly, it samples the surrounding to detect the position of the objective and any obstacles. Secondly, it uses an optimisation algorithm to find the local solution to the optimisation problem [19]. The solution takes the form of the desired direction of movement, which is then fed to the animation controller to move the avatar.

For the purpose of experimental platform validation, a path-follow behaviour was programmed without any obstacles present.

3 PLATFORM VALIDATION

To validate the virtual reality platform, one healthy male test subject (age: 30, height: 191.6 cm, weight: 80.1 kg) was recruited from the cohort of students at the University of Leicester.

Prior to taking part in the experiment, he was asked to: (i) familiarise himself with the participant's information letter, (ii) complete the physical activity readiness questionnaire, and (iii) sign the informed consent form. He was asked to wear flat sole shoes and casual clothing.

The study was approved by the University of Leicester Ethics of Research Committee.

3.1 Location

Due to the space requirement, the Charles Wilson Sports Hall was selected as a suitable location for the validation study. The sports hall is located within the main campus of the University of Leicester, UK. It is 16.7 m wide and 33.5 m long with the clear ceiling height of 5.6 metres at the highest point. To minimise the effect of light reflections on tracking quality, the parquet floor was covered with a dark monotone carpet. This also eliminated visual reference cues offered by the floor markings, which otherwise might have influenced the test subject's movements.

3.2 Experimental protocol

The test subject was provided with a habituation time to familiarise himself with the virtual environment. He was asked to perform a total of sixteen walks around a path consisting of two 10 m long straights and two turns 5 m in diameter. Each walk consisted of 8 laps, resulting in a total distance of 285 m travelled per walk. During each walk, the test subject walked next to (side-by-side; SbS) or behind (front-to-back; FtB) a pacer. The walks were performed in two settings: (i) in the virtual environment (VR), where the pacer was previously created, virtual agent or (ii) in the real environment (RL), where the male performer employed to record virtual agent's motion served as a pacer.

To avoid any directional bias in test subject's behaviour, each walk was performed twice, in a clockwise and an anticlockwise direction around the path. During the first eight walks, the test subject was only directed to maintain his assigned position relative to the pacer, hereafter referred to as uninstructed synchronisation experimental conditions (US). During the last eight walks, the test subject was explicitly asked to walk in step with the pacer, in such manner that the timing of their ipsilateral footsteps was perfectly matched, hereafter referred to as instructed synchronisation experimental conditions (IS).

In order to control real pacer's stepping behaviour, he was equipped with Pioneer SE-M521 over-ear headphones connected to KORG MA-1 metronome. The pacing frequency of the virtual pacer was controlled in the game engine through the animation controller.

The pacing frequency of pacers was based on test subject's height and calculated using the following formula:

$$FR = \frac{v}{gl} \tag{1}$$

where v is the walking velocity, g is the gravitational acceleration, l is a leg length, and FR is the Froude number which was set to 0.15. The leg length l was estimated by using test subject's height, and gender relationship derived by Pheasant [20], and explicitly given by Bocian et al. [21]:

$$l = 0.7028h - 0.3091 \tag{2}$$

where h is the test subject's height. The walking velocity v was converted to the pacing frequency f_p using the Eq. 3, which was derived from experimental data in Soczawa-Stronczyk et al. [22].

$$f_p = 0.66v + 0.99 \tag{3}$$

As a consequence, virtual pacer's pacing frequency was set to 1.81 Hz and the metronome beat for the real pacer was set to 108 BPM.

3.3 Instrumentation

A motion capture system (mocap system) made up of twenty-four OptiTrack Prime 17W and ten OptiTrack Prime 13 cameras was set up in the sports hall. During walks performed in the virtual environment, the test subject was equipped with Oculus Rift CV1 head-mounted display (HMD) together with the MSI VR One 7RE backpack PC used to generate the environment. The HMD had reflective markers affixed to it in order to track its position and rotation using the mocap system. The positional data were wirelessly streamed to the backpack PC from the dedicated mocap processing PC using the NatNet server broadcast protocol version 3.0, through IEEE 802.11n-2009 wireless network.

The virtual environment used during the validation experiment was created using building information modelling (BIM) software - ARCHICAD 23. A high-detail, realistic representation of the Charles Wilson Sports Hall was created.

During all walks, the test subject was instrumented with two APDM Opal™ wireless attitude and heading reference systems (AHRS). One AHRS was attached to the lower back, at the level of fifth lumbar vertebra (L5), whereas the other was strapped to the right ankle, using elastic straps. The data recorded by AHRSs were sampled at 128 Hz and time locked. For the purpose of the subsequent analysis, three-dimensional acceleration signal recorded in the local coordinate system (i.e. sensor) was extracted and resolved to the global coordinate system by means of the quaternion algebra. This allowed the vertical component of the acceleration vector (i.e. that aligned with the gravity vector) to be extracted for further analysis.

The real pacer was outfitted with a set of AHRS of the same type and positioned at the same body locations as in the case of the test subject. This enabled synchronisation to be easily quantified based on a set of compatible signals.

Only the data from the sensor strapped to the ankle were used, as the data were sufficient to describe a gait cycle fully.

Figure 1: A person wearing HMD (right) walking next to the pacer in the virtual environment (left).

As it was impossible to instrument the virtual pacer, the displacement of the right ankle was recorded in the game engine, at a sampling frequency of circa 50 Hz. Considering that the

displacement signal was not time-locked with the AHRS's data, the following time alignment procedure was implemented. An AHRS was fastened to a rigid body with three reflective markers, which were tracked by the motion capture system. The position of the rigid body was isometrically mapped (i.e. preserving distances and rotation angles) onto an unrendered virtual cube, of which displacement was recorded together with the displacement of the virtual pacer's ankle. Before and after each test, the AHRS-rigid body couple was slowly waved using a sinusoidal motion to create a reference signal subsequently used to time-align the data from the game engine and the AHRS.

3.4 Data analysis

The subsequent quantification of the synchronisation strength was performed in MATLAB R2019b and was based on vertical velocity signals from the ankle. This is due to the need to reconcile the displacement signals from the game engine (expressed in m) with the acceleration signals from AHRS (expressed in m/s^2) to a common physical quantity before further processing. In order to minimise the impact of the data loss inherent to the numerical differentiation (high frequency noise), as well as to lessen the signal drift rising from the numerical integration (low frequency noise), it was decided to differentiate game engine's displacement signals and integrate the AHRS' acceleration signals to achieve compatible velocity signals (expressed in m/s), as shown in Figure 2.
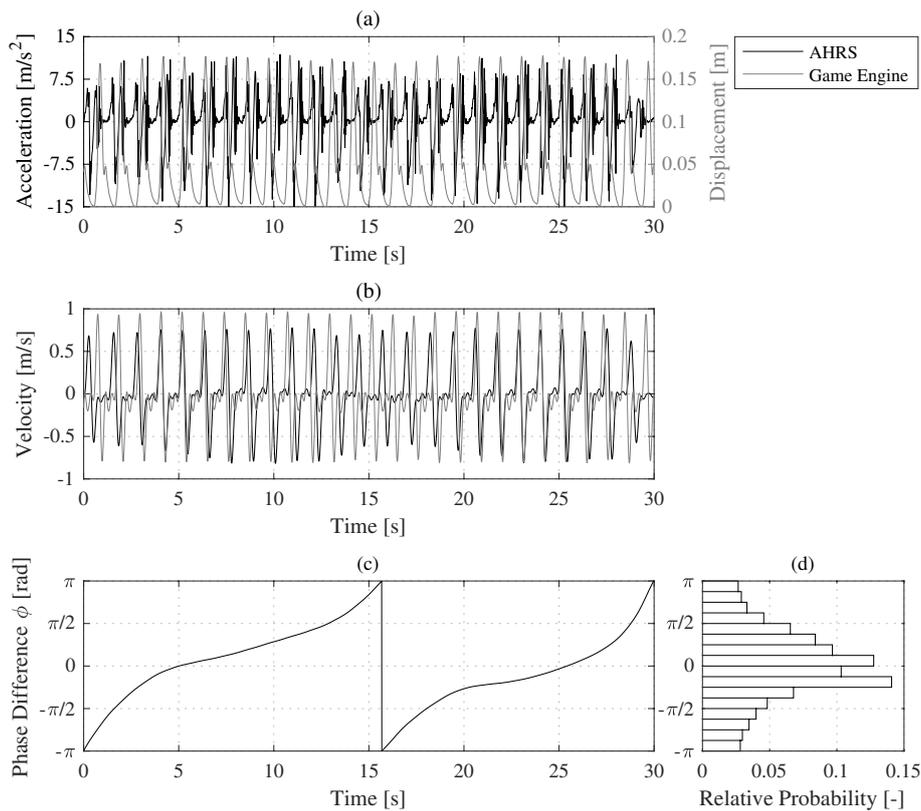
Figure 2: Examples of (a) the raw AHRS acceleration signal and the resampled game engine displacement signal from the ankle, (b) the corresponding velocity signals, (c) the corresponding phase difference signal and (d) the relative probability distribution.

At the start, the displacement signals were upsampled from the variable sampling rate of circa 50 Hz to the uniform sampling rate of 128 Hz to match the sampling rate of AHRS acceleration signals. The upsampling was performed using shape-preserving piecewise cubic interpolation algorithm implemented in MATLAB's *resample* function [23].

In order to differentiate the game engine's displacement signals, a one-dimensional gradient of the vertical displacement vector was calculated and then divided by the numerical gradient of the corresponding time vector. The ensuing velocity vector was post-filtered using the fourth-order two-way Butterworth band-pass filter with the frequency band set to preserve the first three harmonics of the original signal.

The numerical integration of AHRS acceleration signal was proceeded by the pre-filtering of original signals with the fourth-order two-way Butterworth band-pass filter with the same frequency band as in the case of numerical differentiation. The integration was performed by employing the cumulative trapezoidal numerical integration method [24] and post-filtering the resulting velocity signals with the fourth-order two-way Butterworth high-pass filter with the cut-off frequency equal to half of the frequency of the first harmonic.

Finally, with all signals representing the same physical quantity, the two velocity signals derived from the AHRS-rigid body were used to find the delay between AHRS and the game engine's signals for each walk. Using MATLAB's *finddelay* function [25], the cross-correlation between the two velocity signals was calculated at all viable lags. Subsequently, the cross-correlation was normalised, and the estimated delay was given as the negative lag characterised by the largest absolute value of the normalised cross-correlation, which allowed game engine's and AHRS signals to be time-aligned.

3.5 Synchronisation quantification

Before the quantification of pairwise gait synchronisation strength between the test subject and the pacer, analytic representations of velocity signals had to be calculated first. For this purpose, each pair of velocity signals (velocities of test subject's and pacer's right ankles from each walk) was band-pass filtered by utilising the fourth-order two-way Butterworth band-pass filter with a frequency band ranging from 0.70 times the minimum signal (stride) frequency to 1.25 times the maximum stride frequency, as suggested in van Ulzen et al. [26].

For each of the velocity signals $v_i(t)$, the Hilbert transform was then used to obtain the instantaneous phase information contained within the analytic signal $v_i^a(t)$, defined as [27]:

$$v_i^a(t) = v_i(t) + \frac{i}{\pi} P.V. \int_{-\infty}^{+\infty} \frac{v_i(\tau)}{t - \tau} d\tau \tag{4}$$

where $P.V.$ is the Cauchy principal value of the integral. The instantaneous phase angle of the velocity signals $\phi_i(t)$ was calculated by taking the four-quadrant inverse tangent of the imaginary, $\Im$, and real, $\Re$, parts of the analytical signal:

$$\phi_i(t) = \tan^{-1} \frac{\Im[v_i^a(t)]}{\Re[v_i^a(t)]} \tag{5}$$

The phase angle difference of the considered pair of signals $\phi_{p,s}(t)$ was calculated by subtracting test subject's phase angle time series (denoted by subscript s) from the one of the pacer (denoted by subscript p).

$$\phi_{p,s}(t) = \phi_p(t) - \phi_s(t) \tag{6}$$

The synchronisation strength between test subject's and pacer's gait cycles was determined based on the Shannon entropy $E_{p,s}$ of the phase difference distribution, defined as [28]:

$$E_{p,s} = -\sum_{k=1}^{N} P_{p,s}^k \ln P_{p,s}^k \tag{7}$$

where $P_{p,s}^k$ is the probability of the phase difference $\phi_{p,s}(t)$ falling into a kth bin of $\pi/8$ in size, and N is the total number of bins. In order to be able to compare the values of the synchronisation strength across different walks, the synchronisation strength index $\rho_{p,s}$ was then calculated by normalising by the maximum achievable Shannon entropy in the case of the perfect frequency synchrony:

$$\rho_{p,s} = \frac{\ln N - E_{p,s}}{\ln N} \tag{8}$$

The index takes values ranging from 0 to 1, with 0 corresponding to a complete lack of gait synchronisation (i.e. a uniform distribution of phase difference) and 1 representing a perfect gait synchronisation (i.e. a Dirac-like distribution of phase difference).

4 RESULTS AND DISCUSSION

4.1 Stride frequency

In order to assess the influence of the experimental environment on the pacing rate, stride frequency of both pacers and the test subject was calculated using fast Fourier transform for each of the walks. Subsequently, the difference between pacers' and test subject's stride frequencies was quantified. Under US experimental conditions, the mean ($\pm$ standard deviation) difference was equal to $\bar{f}_{p-s}^{RL.US} = 0.060 \pm 0.011$ Hz and to $\bar{f}_{p-s}^{VR.US} = 0.037 \pm 0.008$ Hz during walks in the RL and VR environments, respectively. Similarly, the same comparison made for walks under IS experimental conditions showed an average difference of $\bar{f}_{p-s}^{RL.IS} = 0.004 \pm 0.005$ Hz and $\bar{f}_{p-s}^{VR.IS} = 0.003 \pm 0.002$ Hz, respectively. Moreover, the overall increase of test subject's stride frequency in the virtual environment was equal to 2.81% and 0.13%, under US and IS experimental conditions, respectively. Those results show a high level of affinity between the two tested environments and indicate that test subject's stride frequency remained unaltered in the virtual environment, compared to the real equivalent.

4.2 Gait variability

To evaluate the compatibility of the walking stimulus between the real and virtual environments, the gait cycle variability of both pacers was quantified and assessed through the coefficient of variation (CoV) of the stride frequency.

The mean gait variability attained by the real pacer was $\overline{CoV}_p^{RL} = 1.09 \pm 0.09\%$, with the maximum recorded value of $CoV_p^{RL} = 1.26\%$. The virtual pacer achieved the maximum gait variability of $CoV_p^{VR} = 0.56\%$ with the mean of $\overline{CoV}_p^{VR} = 0.52 \pm 0.03\%$. Even though the average gait variability of the real pacer was double the value achieved by the virtual counterpart, the real pacer's variability was deemed acceptable to provide consistent visual and auditory cues to the test subject. A certain level of discrepancy between the two pacers' gait variabilities was expected due to the inherent inability of the real human to replicate their stepping behaviour perfectly, and the finite number of gait cycles available to drive the virtual pacer.

Under the US experimental conditions, the mean gait variability of the test subject was $\overline{\text{CoV}}_s^{RL.US} = 3.63 \pm 1.44\%$ and $\overline{\text{CoV}}_s^{VR.US} = 3.32 \pm 2.00\%$ during walks in the real and virtual environments, respectively, with the corresponding maximum values $\text{CoV}_s^{RL.US} = 5.43\%$ and $\text{CoV}_s^{RL.US} = 5.75\%$.

The walks performed under IS experimental conditions were characterised by test subject's lower gait variability. The maximum gait variability attained during walks performed in the real and virtual environment, respectively, was $\text{CoV}_s^{RL.IS} = 4.24\%$ and $\text{CoV}_s^{VR.IS} = 3.10\%$, with the mean values of $\overline{\text{CoV}}_s^{RL.IS} = 3.01 \pm 0.95\%$ and $\overline{\text{CoV}}_s^{VR.IS} = 2.31 \pm 0.58\%$ respectively.

The instruction to synchronise steps with the pacer resulted in a decrease in the gait cycle variability in both environments. A more considerable increase in the consistency of the gait cycle was observed during the VR walks, which was pronounced under the IS experimental conditions. This can be attributed to the more isolated conditions offered by the virtual environment. Although the virtual environment was constructed to mimic the sports hall's interior where the tests took place, it secluded the test subject from some of the peripheral stimuli present in the real environment. As a consequence, the test subject's cognitive load was relieved, which might have resulted in more cognitive resources being spent on the execution of gait control. In addition, several studies have reported that the virtual environment alters the distance perception while walking [29–33], resulting in shorter strides [34] and more careful feet placement.

4.3 Synchronisation strength

Synchronisation strength index values achieved during walks under US experimental conditions were comparably low, with the mean synchronisation strength index of $\bar{\rho}^{RL.US} = 0.005 \pm 0.004$ and $\bar{\rho}^{VR.US} = 0.015 \pm 0.014$ during walks performed in the real and virtual environments, respectively, with the corresponding highest index values of $\rho^{RL.US} = 0.012$ and $\rho^{VR.US} = 0.037$.

The synchronisation strength index values recorded under US experimental conditions were below the proposed synchronisation threshold of $\rho = 0.2$ [35]. These results are consistent with previous findings for a pair of walkers [26,36] and a group of pedestrians walking on a rigid ground [22] and a bridge [16], and reflect the transient nature of the unprompted gait adaptation mechanism.

The synchronisation strength index values achieved in IS experimental conditions are presented in Figure 3 (represented by the vector magnitude) and are accompanied by the mean circular direction (represented by the corresponding vector angle) to indicate the directionality of the synchronisation phenomenon. The mean circular direction $\bar{r}$ was calculated by transforming all phase difference values into a two-dimensional vector $\bar{r} = (\cos \alpha, \sin \beta)$ and averaging over the number of data points [37]. According to the adopted sign convention, positive values represent test subject's leading the pacer, and the negative values indicate the test subject lagging the pacer.
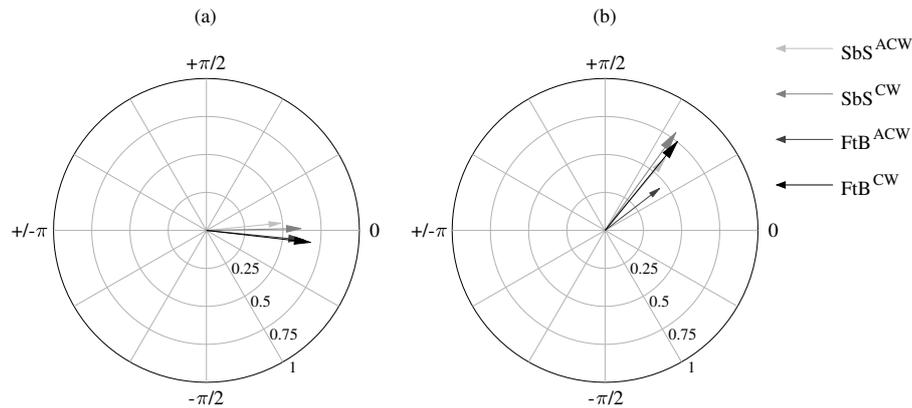
Figure 3: The synchronisation strength index values (magnitude) together with the corresponding mean circular direction (angle) recorded during walks in (a) the real and (b) virtual environments under IS experimental conditions.

The instruction given to the test subject to synchronise his gait cycle with the pacer led to a similar increase in the synchronisation strength values in both environments. The mean synchronisation strength index of $\bar{\rho}^{RL.IS} = 0.605 \pm 0.074$ and $\bar{\rho}^{VR.IS} = 0.650 \pm 0.134$ was attained during walks in the real and virtual environment, respectively. This was the result of the test subject exhibiting increased control over the stepping behaviour in comparison to US walks.

The mean circular direction of the walks performed in the real environment took near-zero values with the front-to-back walks recording slightly negative values, and the side-by-side walks slightly positive values. Negative values of the directionality during front-to-back walks were the result of the test subject reaction to the pacer's action. On the other hand, during side-by-side walks, the pacer was positioned within test subject's horizontal far peripheral vision [38], which might have prompted the emergence of test subject's anticipatory stepping behaviour.

The aforementioned mechanism responsible for the anticipatory behaviour was amplified during the side-by-side walks performed in the virtual environment. This is because of the head-mounted display limiting test subject's horizontal field of view by circa. 110° [39,40], and thus effectively eradicating far peripheral vision. The test subject attempted to compensate for this by falling slightly behind the pacer so that the pacer was within his field of view.

The virtual reality gave rise to an additional mechanism prompting the anticipatory behaviour, as the gait anticipation was also present during the front-to-back walks, where the pacer was no longer positioned in the test subject's far horizontal peripheral but rather in the centre of his gaze. In the front-to-back collocation, the rear walker would attempt to arrive at the double stance phase of gait faster than the person positioned in front in order to allow for a more natural collision avoidance corrections [41].

In the case of side-by-side and front-to-back collocations, the repetitiveness of virtual pacer's gait cycle might have laid grounds for greater predictability of its gait cycle, especially given the more isolated conditions offered by the virtual environment.

5 CONCLUSIONS

This paper presents the development and validation of a novel virtual reality platform for investigating pedestrian-pedestrian interaction and crowd dynamics. The platform utilises the most recent advancements in three-dimensional modelling, motion capturing and virtual reality technology. It comprises of a highly detailed representation of the real environment and an AI-driven virtual pedestrian capable of exhibiting complex social interactions found in real

crowds. The validation process involved a 30 years old male test subject covering the distance in excess of 4 km in the real and virtual environments, walking next to or behind a pacer, that being either a real person or an animated virtual agent. Sixteen walks were recorded in total, including eight without and eight with the instruction to synchronise steps.

No disimilarities were found between test subject's stride frequencies attained in the RL and VR environments, as the stride frequency values increased by a total of 1.42% in the VR. This subsequently resulted in the relationship between test subject's and pacers' stride frequencies being compatible across the two tested environments.

The assessment of the difference between test subject's and pacers' stride frequencies yielded compatible results in both, the real and virtual environments. Furthermore, no significant differences in gait parameters of the tested subject were found between the two tested environments.

The analysis of pacers' gait variability showed that the average difference between real and virtual pacers' gait variability is equal to 0.57%, which ensures the compatibility of the visual and auditory cues provided by the walking stimulus across the two environments. The test subject's gait variability was lower in the virtual environment by 8.5% under US experimental conditions, and by 23.3% under IS experimental conditions. The more consistent stepping behaviour was likely the result of a smaller number of peripheral stimuli offered by the virtual environment, which subsequently allowed for a greater focus on pacer's motion.

Under US experimental conditions, the synchronisation strength index achieved in the virtual reality platform was compatible with the real environment, yielding values not exceeding 0.04. This is consistent with previous results obtained for a pair of walkers [26,36] and during walking in a group [16,22].

The instruction given to the test subject to synchronise his gait with that of the pacer resulted in an increase of the synchronisation strength index in both environments beyond 0.2. The effect of the instruction was stronger in the virtual environment, where the synchronisation strength index was higher by 7.4%. The directionality of gait synchronisation revealed that in the real environment, the test subject was reacting to pacer's stepping behaviour during walks in the front-to-back arrangement and anticipating pacer's footsteps during side-by-side walks. The anticipatory behaviour was further amplified in the virtual environment and also emerged during front-to-back walks.

Overall, the preliminary results presented herein indicate that the developed experimental platform has the potential to become a viable solution for investigating crowd dynamics, within and beyond the context of vibration serviceability.

ACKNOWLEDGEMENTS

REFERENCES

[1]   Venuti F, Bruno L. Crowd-structure interaction in lively footbridges under synchronous lateral excitation: A literature review. Phys Life Rev 2009;6:176–206. https://doi.org/10.1016/j.plrev.2009.07.001.

[2]   Dallard P, Fitzpatrick T, Flint A, Low A, Smith RR, Willford M, et al. London Millennium Bridge: Pedestrian-Induced Lateral Vibration. J Bridg Eng 2001;6:412–7. https://doi.org/10.1061/(ASCE)1084-0702(2001)6:6(412).

[3] Dallard P, Fitzpatrick AJ, Flint A, Le Bourva S, Low A, Ridsdill Smith RM, et al. The London Millennium Footbridge. Struct. Eng., 2001.

[4] Brownjohn JMW, Fok P, Roche M, Moyo P. Long span steel pedestrian bridge at Singapore Changi Airport - Part 1: Prediction of vibration serviceability problems. Struct Eng 2004.

[5] Brownjohn JMW, Fok P, Roche M, Omenzetter P. Long span steel pedestrian bridge at Singapore Changi Airport - Part 2: Crowd loading tests and vibration mitigation measures. Struct Eng 2004.

[6] Caetano E, Cunha Á, Magalhães F, Moutinho C. Studies for controlling human-induced vibration of the Pedro e Inês footbridge, Portugal. Part 1: Assessment of dynamic behaviour. Eng Struct 2010;32:1069–81. https://doi.org/10.1016/j.engstruct.2009.12.034.

[7] Caetano E, Cunha Á, Moutinho C, Magalhães F. Studies for controlling human-induced vibration of the Pedro e Inês footbridge, Portugal. Part 2: Implementation of tuned mass dampers. Eng Struct 2010;32:1082–91. https://doi.org/10.1016/j.engstruct.2009.12.033.

[8] Kawasaki T, Nakamura S, Ohno K. Field measurement of lateral vibration of a suspension bridge induced by pedestrians. Doboku Gakkai Ronbunshu 2004;2004:97–107. https://doi.org/10.2208/jscej.2004.777_97.

[9] Nakamura S ichi, Kawasaki T. Lateral vibration of footbridges by synchronous walking. J Constr Steel Res 2006;62:1148–60. https://doi.org/10.1016/j.jcsr.2006.06.023.

[10] Hoorpah W, Flamand O, Cespedes X. The Simone de Beauvoir Footbridge between Bercy Quay and Tolbiac Quay in Paris: Study and measurement of the dynamic behaviour of the structure under pedestrian loads and discussion of corrective modifications. In: Caetano E, Cunha Á, Hoorpah W, Raoul J, editors. Footbridge Vib. Des. 1st Editio, Leiden, The Netherlands: CRC Press/Balkema; 2017, p. 202.

[11] Bocian M, Burn JF, Macdonald JHG, Brownjohn JMW. From phase drift to synchronisation – pedestrian stepping behaviour on laterally oscillating structures and consequences for dynamic stability. J Sound Vib 2017;392:382–99. https://doi.org/10.1016/j.jsv.2016.12.022.

[12] Grundmann H, Kreuzinger H, Schneider M. Dynamic calculation of footbridges. Bauingenieur 1993;68:215–25.

[13] Piccardo G, Tubino F. Parametric resonance of flexible footbridges under crowd-induced lateral excitation. J Sound Vib 2008. https://doi.org/10.1016/j.jsv.2007.09.008.

[14] Newland DE. Pedestrian excitation of bridges. Proc Inst Mech Eng Part C J Mech Eng Sci 2004. https://doi.org/10.1243/095440604323052274.

[15] Venuti F, Bruno L, Napoli P. Pedestrian Lateral Action on lively Footbridges: A New Load Model. Struct Eng Int 2007;17:236–41. https://doi.org/10.2749/101686607781645897.

[16] Bocian M, Brownjohn JMW, Racic V, Hester D, Quattrone A, Gilbert L, et al. Time-dependent spectral analysis of interactions within groups of walking pedestrians and vertical structural motion using wavelets. Mech Syst Signal Process 2018;105:502–23. https://doi.org/10.1016/j.ymssp.2017.12.020.

[17] Pimentel RL, Araújo MC, Brito HMBF, de Brito JLV. Synchronization among Pedestrians in Footbridges Due to Crowd Density. J Bridg Eng 2013;18:400–8. https://doi.org/10.1061/(ASCE)BE.1943-5592.0000347.

[18] Van Nimmen K, Lombaert G, Jonkers I, De Roeck G, Van den Broeck P. Characterisation of walking loads by 3D inertial motion tracking. J Sound Vib 2014;333:5212–26. https://doi.org/10.1016/J.JSV.2014.05.022.

[19] Polarith UG. Polarith AI Documentation 2019. http://docs.polarith.com/ai/index.html (accessed January 29, 2020).

[20] Pheasant ST. Anthropometric estimates for british civilian adults. Ergonomics 1982;25:993–1001. https://doi.org/10.1080/00140138208925060.

[21] Bocian M, Macdonald JHG, Burn JF. Probabilistic criteria for lateral dynamic stability of bridges under crowd loading. Comput Struct 2014;136:108–19. https://doi.org/10.1016/j.compstruc.2014.02.003.

[22] Soczawa-Stronczyk AA, Bocian M, Wdowicka H, Malin J. Topological assessment of gait synchronisation in overground walking groups. Hum Mov Sci 2019;66:541–53. https://doi.org/10.1016/j.humov.2019.06.007.

[23] MathWorks. Resample uniform or nonuniform data to new fixed rate - MATLAB resample 2019. https://uk.mathworks.com/help/signal/ref/resample.html (accessed February 20, 2020).

[24] Venkateshan SP, Swaminathan P. Numerical Integration. Comput. Methods Eng., Elsevier; 2014, p. 317–73. https://doi.org/10.1016/b978-0-12-416702-5.50009-0.

[25] MathWorks. Estimate delay(s) between signals - MATLAB finddelay 2019. https://uk.mathworks.com/help/signal/ref/finddelay.html (accessed January 14, 2020).

[26] van Ulzen NR, Lamoth CJC, Daffertshofer A, Semin GR, Beek PJ. Characteristics of instructed and uninstructed interpersonal coordination while walking side-by-side. Neurosci Lett 2008;432:88–93. https://doi.org/10.1016/j.neulet.2007.11.070.

[27] Rosenblum MG, Pikovsky AS, Kurths J. Phase synchronization of chaotic oscillators. Phys Rev Lett 1996;76:1804–7. https://doi.org/10.1103/PhysRevLett.76.1804.

[28] Tass P, Rosenblum MG, Weule J, Kurths J, Volkmann J, Schinitzler A, et al. Detection of n: m phase locking from noisy data: application to magnetoencephalography. Phys Rev Lett 1998;81:3291–4.

[29] Janeh O, Langbehn E, Steinicke F, Bruder G, Gulberti A, Poetter-Nerger M. Walking in virtual reality: Effects of manipulated visual self-motion on walking biomechanics. ACM Trans Appl Percept 2017;14. https://doi.org/10.1145/3022731.

[30] Steinicke F, Bruder G, Jerald J, Frenz H, Lappe M. Estimation of detection thresholds for redirected walking techniques. IEEE Trans Vis Comput Graph 2010. https://doi.org/10.1109/TVCG.2009.62.

[31] Knapp J, Loomis J. Visual Perception of Egocentric Distance in Real and Virtual Environments. Virtual Adapt. Environ., CRC Press; 2003, p. 21–46. https://doi.org/10.1201/9781410608888.pt1.

[32] Renner RS, Velichkovsky BM, Helmert JR. The Perception of Egocentric Distances in Virtual Environments - A Review. ACM Comput Surv 2013;46. https://doi.org/10.1145/2543581.2543590.

[33] Willemsen P, Colton MB, Creem-Regehr SH, Thompson WB. The effects of head-mounted display mechanics on distance judgments in virtual environments. Proc. 1st Symp. Appl. Percept. Graph. Vis. - APGV '04, New York, New York, USA: ACM Press; 2004, p. 35. https://doi.org/10.1145/1012551.1012558.

[34] Mohler BJ, Campos JL, Weyel MB, Bülthoff HH. Gait parameters while walking in a head-mounted display virtual environment and the real world. Proc. 13th Eurographics Symp. Virtual Environ., 2007. https://doi.org/10.2312/PE/VE2007Short/085-088.

[35] Zivotofsky AZ, Gruendlinger L, Hausdorff JM. Modality-specific communication enabling gait synchronization during over-ground side-by-side walking. Hum Mov Sci 2012;31:1268–85. https://doi.org/10.1016/j.humov.2012.01.003.

[36] van Ulzen NR, Lamoth CJC, Daffertshofer A, Semin GR, Beek PJ. Stability and variability of acoustically specified coordination patterns while walking side-by-side on a treadmill: Does the

seagull effect hold? Neurosci Lett 2010;474:79–83. https://doi.org/10.1016/J.NEULET.2010.03.008.

[37]   Berens P. CircStat: A MATLAB toolbox for Circular Statistics. J Stat Softw 2009;31:1–21. https://doi.org/10.18637/jss.v031.i10.

[38]   Simpson MJ. Mini-review: Far peripheral vision. Vision Res 2017;140:96–105. https://doi.org/10.1016/j.visres.2017.08.001.

[39]   Rakkolainen I, Raisamo R, Turk M, Hollerer T, Palovuori K. Extreme field-of-view for head-mounted displays. 3DTV-Conference, vol. 2017- June, IEEE Computer Society; 2018, p. 1–4. https://doi.org/10.1109/3DTV.2017.8280417.

[40]   Howell HW. Medical Physiology and Biophysics. London, UK: Sounders; 1960.

[41]   Repp BH, Su Y-H. Sensorimotor synchronization: A review of recent research (2006–2012). Psychon Bull Rev 2013;20:403–52. https://doi.org/10.3758/s13423-012-0371-2.